Polym. Bull. (2010) 64:749–759
DOI 10.1007/s00289-009-0167-3

ORIGINAL PAPER

Synthesis of linear low density polyethylene with a nano-sized silica supported Cp_2ZrCl_2/MAO catalyst

Kuo-Tseng Li · Chi-Lun Dai · Cheng-Yu Li

Received: 10 September 2008 / Revised: 31 August 2009 / Accepted: 21 September 2009 /
Published online: 11 October 2009

Abstract A nano-sized silica supported Cp_2ZrCl_2/MAO catalyst was used to catalyze the copolymerization of ethylene/1-hexene and ethylene/1-octene to produce linear low-density polyethylene (LLDPE) in a batch reactor. Under identical reaction conditions, the nano-sized catalyst exhibited significantly higher polymerization activity, and produced copolymer with greater molecular weight and smaller polydispersity index than a corresponding micro-sized catalyst, which was ascribed to the much lower internal diffusion resistance of the nano-sized catalyst. Copolymer density decreased with the increase of polymerization temperature, probably due to the decrease of reactivity ratio r_1 and ethylene solubility with increasing temperature. Polymerization activity of the nano-sized catalyst increased rapidly with increasing comonomer concentration. Ethylene/1-octene exhibited higher polymerization activity and had a stronger comonomer effect than ethylene/1-hexene.

Keywords Linear low density polyethylene · Supported metallocene/MAO catalyst · Ethylene-1-hexene copolymerization · Ethylene-1-octene copolymerization · Nano silica particles

Introduction

Linear low-density polyethylene (LLDPE) is a large volume commodity product with worldwide production quantities of over 15×10^6 metric tons/year. It is widely used in films (the largest single market for LLDPE resins), pipe/tubing, bottles/containers, electric wire, and cable insulation [1, 2]. LLDPE is a copolymer

K.-T. Li (✉) · C.-L. Dai · C.-Y. Li
Department of Chemical Engineering and Materials Engineering, Tunghai University, Taichung, Taiwan, ROC
e-mail: ktli@thu.edu.tw

of ethylene and α-olefins. The use of α-olefins as a comonomer affects the density due to the side-chain branching. Four olefins are used in industry to manufacture LLDPE: 1-butene, 1-hexene, 4-methyl-1-pentene, and 1-octene. Ethylene-1-hexene and ethylene-1-octene copolymers exhibit film properties which are superior to those of ethylene-1-butene copolymer [1].

The LLDPE resins are produced in industry with three classes of catalysts: Ziegler catalysts, metallocene-based catalysts (Kaminsky and Dow), and chromium oxide-based catalysts (Phillips) [1]. Catalytic systems influence the structure and properties of the copolymer. Metallocene catalysts activated by methylaluminoxane (MAO) show very high activity in ethylene copolymerization and produce uniform polymer with narrow molecular weight distribution and narrow comonomer distribution [3–5]. A LLDPE with uniform ethylene-α-olefin composition produced with metallocene catalysts, was first introduced by Exxon Chemical Co. in 1990. The growth of metallocene-based LLDPE is rapid, and a remarkable part of the LLDPE produced worldwide is made by metallocene catalysts [5].

Many metallocene catalysts have been supported on inorganic carriers, typically silica, for industrial use [6–11]. The development of supported metallocenes is crucial for industrial application because it enables their use in gas- and slurry-phase processes and prevent reactor-fouling problems. It also enables the formation of uniform particles with narrow size distribution and high bulk density.

In the literature, the sizes of silica particles used to support metallocene/MAO catalysts for ethylene copolymerization to LLDPE were usually in the range of micrometers [12–14], where most active sites for polymerization were located inside fine pores, and strong internal diffusion resistance might occur inside the pores of the micro-sized catalysts.

Nano-sized particles had a characteristic of very large external specific surface areas. Recently, we found that nano-sized silica-supported metallocene catalysts had better activity for propylene polymerization and for ethylene homopolymerization than micro-sized silica-supported metallocene catalyst [15–17].

In this study, a nano-sized silica particle was used as the support for bis(cyclopentadienyl) zirconium (IV) dichloride (abbreviated as Cp_2ZrCl_2)/MAO catalyst. The nano-sized catalyst system was used to catalyze the copolymerization of ethylene/1-hexene and ethylene/1-octene. We found that the nano-sized catalyst exhibited much better copolymerization activity than a micro-sized catalyst system under identical reaction conditions. In addition, polymers produced with the nano-sized catalyst had greater molecular weight and lower polydispersity index than those produced with the micro-sized catalyst.

Experimental

Catalyst preparation and characterization

Two silica sources were used for supporting Cp_2ZrCl_2/MAO catalyst. One silica was nano-sized, supplied by SeedChem (Melbourne, Australia); another silica was micro-sized, supplied by Strem (Newburyport, MA, USA). Transmission electron

micrograph indicated that nano-sized silica particle had a length of around 10 nm and a width of around 4 nm [15]. Scanning electron micrograph indicated that micro-sized silica particle had a size of around 100 μm [15].

The silica-supported Cp_2ZrCl_2/MAO catalysts were prepared using a method reported previously [16, 18], according to the following procedure: (1) calcination of silica particles at 450 °C under a nitrogen flow (10^{-4} m^3/min) for 4 h; (2) immobilization of MAO on the supports by heating 3×10^{-6} m^3 10 wt% MAO solution (in toluene) with 5×10^{-4} kg silica particle at 50 °C for 24 h, followed by washing with toluene; (3) reaction of the MAO-treated supports with metallocene compounds (7.5×10^{-6} kg Cp_2ZrCl_2) at 70 °C for 24 h, followed by washing with toluene; and (4) drying the catalyst at 50 °C. The operations of steps from (2) to (4) were carried out under a dry argon atmosphere by using glove-box technique. Cp_2ZrCl_2 and MAO (10 wt% solution in toluene) were supplied by Strem (Newburyport, MA, USA) and Albemarle (Baton Rouge, LA, USA), respectively. Zirconium and aluminum contents of the resulting supported metallocene/MAO catalysts were determined with an inductively coupled plasma–atomic emission (ICP–AES) spectrometer (Kontron, Model S-35) after HF acid digestion of the solid. The specific surface areas of the silica samples were determined by nitrogen adsorption at the temperature of liquid nitrogen with a Micrometrics BET surface area analyzer (Model ASAP 2020). BET measurements indicated that the surface areas were 582,000 and 305,000 m^2/kg for nano-sized silica and micro-sized silica, respectively. ICP measurements indicated that Zr contents were 0.6 and 0.9 wt% for nano-sized catalyst and micro-sized catalyst, respectively [16], Al contents were 10.3 and 9.8 wt% for nano-sized catalyst and micro-sized catalyst, respectively.

Ethylene copolymerization and polymer characterization

A 3×10^{-4} m^3 high-pressure autoclave reactor (supplied by Parr Instrument Co.) equipped with an impeller and a temperature control unit was employed for carrying out the catalytic copolymerization of ethylene-1-hexene and ethylene-1-octene. In a typical experiment, 1×10^{-4} m^3 toluene, 5×10^{-6} kg supported Cp_2ZrCl_2/MAO catalysts (prepared by impregnation method mentioned above), and 3×10^{-6} m^3 MAO solution were charged to the reactor. The reactor was heated to the desired temperature (the temperature was set in the range of 40–80 °C). Ethylene at 550 kPa and a specific amount of 1-hexene/1-octene were then introduced simultaneously into the reactor to initiate the polymerization, and the reactor inlet valves were then closed. The agitator speed was set at 400 rpm, and the reaction time was 1 h. The copolymerization was then terminated by adding acidic methanol and the polymer product was dried in a vacuum oven. The measured polymer weight was used for determining the polymerization activity according to the following equation: polymerization activity = (kilograms of LLDPE)/(polymerization time × kg mol of Zr in the catalyst). DSC measurements for the determination of polymer melting point were carried out on a differential scanning calorimeter (Perkin Elmer Pyris-1) with a heating rate of 10 °C/min. Polymer density was measured with an electronic densimeter (Mirage SD-120L). Polymer molecular weight and molecular weight distribution were determined by high-temperature gel

permeation chromatography (GPC) using a Waters alliance GPCV20000 system equipped with three columns (2 Styragel HT6E and 1 Styragel HT2) at 135 °C. *O*-dichlorobenzene was used as the mobile phase. A calibration curve was established using monodispersed polystyrene standards.

Results and discussion

Figure 1 compares the difference in polymerization activity between nano-sized catalyst and micro-sized catalyst in the temperature range of 40–80 °C, which was obtained with the copolymerization of ethylene and 1-hexene at a 1-hexene concentration of 0.28 kg mol/m^3. Figure 1 indicates that polymerization activities of nano-sized catalyst (curve a) were significantly higher than (1.7–2.7 times) those of micro-sized catalyst (curve b). Both the curves (a) and (b) exhibit a volcano shape with a maximum polymerization activity at the polymerization temperature of 60 °C. Below and above the optimum temperature, polymerization activity decreased. The maximum polymerization activities obtained for nano-sized catalyst and micro-sized catalyst were 6.1 × 10^5 and 3.5 × 10^5 kg LLDPE/kg mol Zr h, respectively. That is, the maximum activity obtained (at 60 °C) with nano-sized catalyst was 1.74 times that obtained with micro-sized catalyst.

The global polymerization rate, R_p, in Ziegler–Natta catalysis and metallocene catalysis, is generally represented by [15]:

$$R_p = k_p[C^*][M] \quad (1)$$

where k_p is the propagation rate constant, [C^*] is the catalytic active species concentration, and [M] is the monomer concentration. The concentration of catalytic active species in Eq. 1 is related to polymerization time, t [15]

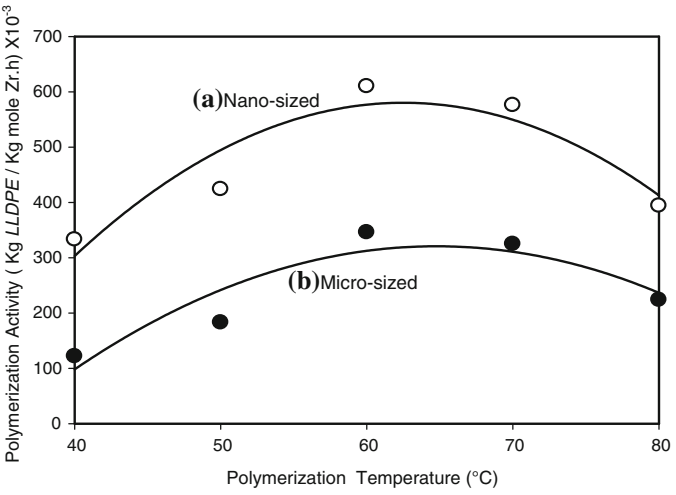

Fig. 1 Polymerization activity as a function of polymerization temperature for (*a*) nano-sized catalyst and (*b*) micro-sized catalyst

$$[C^*] = [C^*]_o \exp\ (-k_d\, t) \tag{2}$$

where $[C^*]_o$ is the initial concentration of the catalytic active species, k_d is the deactivation rate constant. The volcano shape that appeared, Fig. 1, might be attributed to increase in the rates of both propagation ($k_p = k_{p0}\ \exp[-E_p/RT]$) and catalyst deactivation ($k_d = k_{d0}\ \exp[-E_d/RT]$), and the decrease of ethylene solubility in toluene (i.e., $[M]$) [19] with increasing temperature.

Nano-sized silica had a length of 10 nm and a width of 4 nm, and, therefore, most of the nano-sized silica surface areas were external surface areas, and active sites on the nano-sized catalyst external surface should be free from internal diffusion resistance [16]. In the region of no internal diffusion resistance, polymerization rate is independent of particle size [20]; therefore, the further decrease of particle sizes (smaller than 10 nm) cannot produce higher rates. On the contrary, almost all of the micro-sized silica surface areas were internal (i.e., inside the pores) surface areas, and active sites on the internal surface might have strong diffusion resistance. Therefore, nano-sized catalyst's active sites had higher reactant concentration (i.e., $[M]$ in Eq. 1) than micro-sized catalyst's active sites, which resulted in the higher polymerization rates for the former, as shown in Fig. 1.

Zheng et al. [21] determined aluminum distribution in a MAO-impregnated silica support (with a particle size of 50 μm) by using energy-dispersive X-ray (EDX) analysis. They found that MAO was homogeneously distributed on the support when silica was impregnated with MAO at elevated temperature. The results of Zheng et al. prove that most active sites of micro-sized catalyst were inside the silica pores.

It is also possible that other properties of the two supports besides the size, such as acidity (i.e., the number of surface SiOH groups) and other surface properties, might affect the polymerization activity. Our FTIR measurements indicated that surface SiOH concentration of calcined nano-sized silica was 26% higher than that of calcined micro-sized silica. The SiOH concentration difference might be due to the surface energy difference between micron and nano silica.

Figure 2 shows polymer weight-averaged molecular weight (denoted as $\overline{M_W}$) as a function of polymerization temperature. Under identical polymerization conditions, nano-sized catalyst produced LLDPE with significantly higher molecular weight than micro-sized catalyst did. Figure 2 also shows that the molecular weight of the copolymer produced with the nano-sized catalyst decreased from 3.1×10^5 to 1.3×10^5 kg/kg mol on raising the polymerization temperature from 40 to 80 °C.

For a homogeneous polymerization catalyst, it was proposed that [22]

$$1/\overline{P_n} = (k_{TM}/k_P)(1/[M]) + k_{TO}/k_p \tag{3}$$

where $\overline{P_n}$ is the degree of polymerization (= number-averaged molecular weight/monomer molecular weight), $[M]$ is the monomer concentration, k_P is the propagation rate constant, k_{TM} is the chain termination rate constant due to β–H transfer to the metal, and k_{TO} is the chain termination rate constant due to β–H transfer to an olefin. The decrease of molecular weight with the increase of polymerization temperature (shown in Fig. 2) should be because of the enhanced chain-transfer reactions. That is, k_{TM}/k_P or k_{TO}/k_p increased with increasing

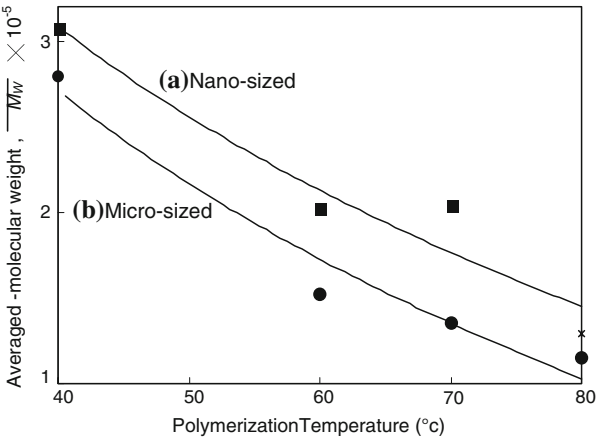

Fig. 2 Effect of polymerization temperature on molecular weight of ethylene-1-hexene copolymers produced with (*a*) nano-sized catalyst and (*b*) micro-sized catalyst

polymerization temperature because the activation energies for chain-transfer reactions (E_{TM} and E_{TO}) are greater than the activation energy for propagation reaction [15].

Equation 3 also indicates that the higher the monomer concentration [*M*], the higher the molecular weight of the polymer produced. Therefore, the higher molecular weight observed for the polymer produced with the nano-sized catalyst (shown in Fig. 2) should be caused by the higher monomer concentration at the active sites of the nano-sized catalyst. As mentioned above, nano-sized catalyst's active sites were located at the external surface and had no internal diffusion resistance, whereas micro-sized catalyst's active sites were located inside the pores and had strong internal diffusion resistance. Therefore, the external active sites on nano-sized catalyst had higher monomer concentration than the internal active sites on micro-sized catalyst, and thus produced copolymers with higher molecular weight.

Figure 3 shows the effect of polymerization temperature on polydispersity index (PDI = weight-averaged molecular weight/number-averaged molecular weight) for (a) nano-sized catalyst and (b) micro-sized catalyst. At the same polymerization temperature, nano-sized catalyst produced polymers with polydispersity values significantly lower than those produced with micro-sized catalyst. PDI increased from 1.46 to 2.25 with increasing polymerization temperature for the polymers produced using the nano-sized catalyst.

Figure 4 compares GPC chromatograms of LLDPE obtained with (a) nano-sized catalyst and (b) micro-sized catalyst at the polymerization temperature of 70 °C. As it may be seen, curve (b) is broader than curve (a), and curve (b) is characterized by a bimodal distribution. Figures 3 and 4 indicate that nano-sized catalyst produced polymers with smaller PDI than micro-sized catalyst did. It is known that in the presence of internal diffusion limitation, even if all sites were chemically identical, polymer chains with different PDI would be produced at different radial positions,

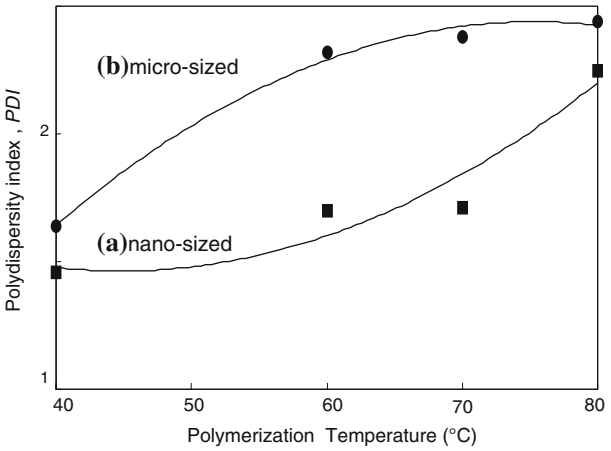

Fig. 3 Ethylene-1-hexene copolymer polydispersity index as a function of polymerization temperature for (*a*) nano-sized catalyst and (*b*) micro-sized catalyst

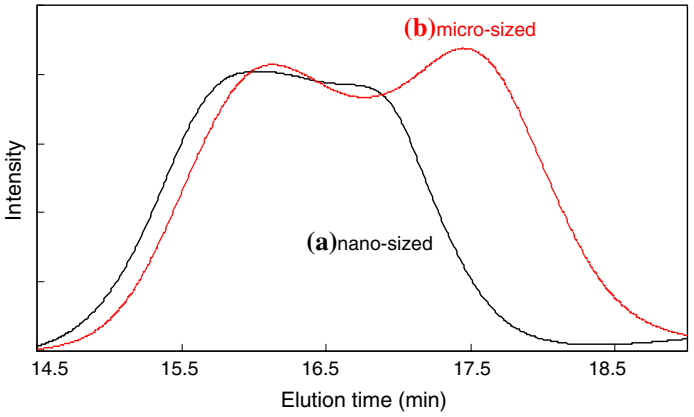

Fig. 4 GPC chromatograms of ethylene-1-hexene copolymers obtained with (*a*) nano-sized catalyst and (*b*) micro-sized catalyst at the polymerization temperature of 70 °C

and thus a rather wide overall PDI would result [23]. Therefore, the larger PDI obtained for the polymers produced with micro-sized catalyst provided additional evidence proving that the micro-sized catalyst had significant internal diffusion resistance. Confinement effects might exist because our SEM micrographs [16] showed that nano-polyethylene fibers was produced (the sign of polymer extrusion) with the use of nano-sized catalyst. Therefore, confinement effects of ethylene polymerization might also affect the PDI of LLDPE. The lower PDI of LLDPE obtained with nano-sized catalyst might also partly be due to its less particle size distribution. As observed with our SEM and the TEM micrographs reported elsewhere [15], nano-sized silica had less particle size distribution than micro-sized silica.

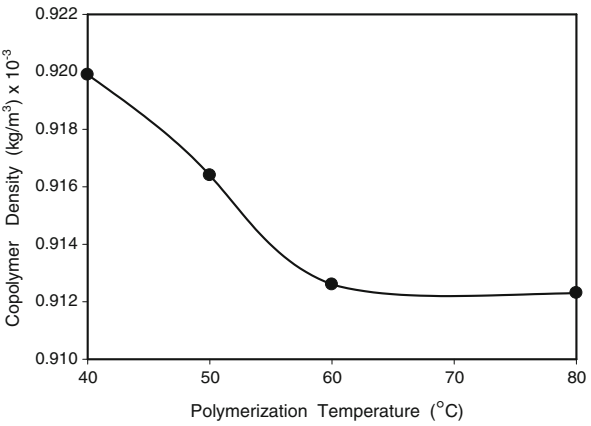

Fig. 5 Ethylene-1-hexene copolymer density as a function of polymerization temperature for the nano-sized catalyst

Figure 5 indicates that ethylene-1-hexene copolymer density produced with nano-sized catalyst decreased generally with increasing polymerization temperature, and the density was in the range of 912–920 kg/m^3. It was reported that LLDPE density was 918–920 kg/m^3 for 2 mol% 1-hexene content, and was 908–912 kg/m^3 for 3 mol% 1-hexene content [1].

The mole ratio of monomer M_1 (ethylene) and M_2 (1-hexene) contained in a copolymer is given by the following copolymerization equation [24]:

$$\mathrm{d}[M_1]/\mathrm{d}[M_2] = \{[M_1](r_1[M_1] + [M_2])\}/\{[M_2]([M_1] + r_2[M_2])\} \quad (4)$$

The copolymer composition $\mathrm{d}[M_1]/\mathrm{d}[M_2]$ is the molar ratio of the two monomer units in the copolymer, and $[M_1]$ and $[M_2]$ are instantaneous concentrations of the two monomers in the reaction solution. The decrease of copolymer density with increasing polymerization temperature (shown in Fig. 5) indicating that $\mathrm{d}[M_1]/\mathrm{d}[M_2]$ decreased with increasing polymerization temperature. That is, more 1-hexene was incorporated into the copolymer at the higher temperature.

In the case of homogeneous Cp_2ZrCl_2/MAO catalyst-catalyzed ethylene-1-hexene copolymerization, the reactivity ratio r_1 ($=k_{11}/k_{12}$) decreased with increasing polymerization temperature in the temperature range of 20–60 °C (r_1 = 55, 54, 52 at 20, 40, and 60 °C, respectively), and r_2 ($=k_{22}/k_{21}$) was not sensitive to the temperature change [25]. Therefore, there are two possible reasons for the decrease of $\mathrm{d}[M_1]/\mathrm{d}[M_2]$ with increasing polymerization temperature (shown in Fig. 5): (1) the decrease of r_1 with polymerization temperature [25], (2) the rapid decrease of ethylene solubility in toluene (i.e., $[M_1]$ in Eq. 4) with increasing temperature [19].

Figure 6 shows the variation of polymerization activities as a function of comonomer (1-hexene and 1-octene) concentration for the nano-sized catalyst at the polymerization temperature of 60 °C. The feed ratio of ethylene/1-hexene was in the range of 3.05–11, and that of ethylene/1-octene was in the rage of 2.3–8.7. For both 1-hexene and 1-octene, polymerization activities increased with increasing

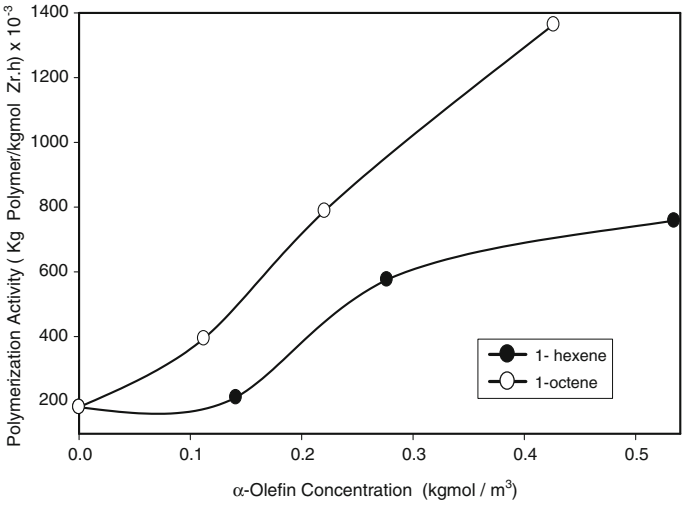

Fig. 6 Polymerization activity as a function of comonomer concentration for ethylene-1-hexene and ethylene-1-octene copolymerization with nano-sized catalyst

comonomer concentration. DSC measurements indicated that the copolymer melting temperature, T_m, was in the range of 128–113 °C. ^{13}C-NMR measurements indicated that the copolymers contained 1–3 mol% of α-olefin.

The result shown in Fig. 6 (that ethylene-1-octene has higher polymerization activity than ethylene-1-hexene at the same comonomer concentration) is consistent with the results of Hong et al. [3]. These authors used a homogeneous (unsupported) constrained geometry $[(\eta_5\text{-}C_5Me_4)SiMe_2(\eta_1\text{-}NCMe_3)]TiCl_2$ catalyst to catalyze the copolymerization of ethylene-1-decene/ethylene-1-octene/and ethylene-1-hexene, and found that the catalyst activity increased with the increase of comonomer content and had the following general trend: 1-decene > 1-octene > 1-hexene. The activity difference observed in Fig. 6 might be due to the higher boiling point of 1-octene (b.p. of 1-octene = 122 °C, b.p. of 1-hexene = 63 °C), which maintained higher concentration of 1-octene in the reaction solution [3].

Based on Raoult's law and vapor pressure data of 1-hexene/1-octene at 60 °C [26], the calculated K_i values ($K_i = y_i/x_i$ = mole fraction of species i in the gas mixture/mole fraction of species i in the liquid mixture) at 550 kpa (polymerization pressure) were 0.164 and 0.0031 for 1-hexene and 1-octene, respectively. That is, 1-octene concentration in the liquid phase was about 15% higher than 1-hexene, which resulted in the higher polymerization activity and stronger comonomer effect for 1-octene.

The effect of comonomer type on polymerization activity observed for micro-sized catalyst was less significant than that shown in Fig. 6. At the α-olefin concentration of 0.43 kg mol/m^3, the micro-sized catalyst activity for ethylene-1-octene copolymerization was only 1.05 times that for ethylene-1-hexene copolymerization, which was less than that (∼2 times) observed for the nano-sized catalyst. The results we obtained with micro-sized catalyst (less effect of comonomer effect) are consistent with the micro-sized silica-supported Cp_2ZrCl_2/

MAO catalyst results obtained by Awudza and Tait [14]. They found only a slight variation of CEF values with the type of comonomer used, where CEF is the abbreviation of "comonomer effect factor" and CEF is the ratio of average polymerization rate for copolymerization to average polymerization rate for homopolymerization. In the micro-sized catalyst (with strong internal diffusion resistance), 1-octene is more difficult (compared to 1-hexene) to reach the active sites because it has the lower diffusivity (due to its larger molecular weight). Therefore, the higher 1-octene concentration in the liquid reaction solution (compared to 1-hexene, due to the higher boiling point of 1-octene) is nullified by the lower 1-octene diffusivity in the micro-sized catalyst.

Conclusions

A nano-sized silica supported Cp_2ZrCl_2/MAO catalyst was used to catalyze the copolymerization of ethylene-1-hexene and the copolymerization of ethylene-1-octene to synthesize LLDPE. Under identical reaction conditions, the polymerization activity of the nano-sized catalyst was over 1.7 times that of a micro-sized catalyst. Polymers produced with nano-sized catalyst had higher molecular weight and narrower molecular weight distribution than those produced with micro-sized catalyst. The superiority of the nano-sized catalyst should be caused by the fact that most of its active sites were located at the exterior surface, which were free from internal diffusion resistance. For the nano-sized catalyst-catalyzed copolymerization, ethylene-1-octene system had higher polymerization activity and had stronger comonomer effect than ethylene-1-hexene system.

Acknowledgment The authors are grateful to National Science Council of *ROC* for their financial support (NSC-94-2214-E029-002).

References

1. Kissin YV (1996) Linear low density polyethylene. In: Kroschwitz JI, Howe-Grant M (eds) Encyclopedia of chemical technology, vol 17, 4th edn. Wiley, New York, pp 756–784
2. James DE (1987) Linear low density polyethylene. In: Kroschwitz JI (ed) Encyclopedia of polymer science and engineering, vol 6, 2nd edn. Wiley, New York, pp 429–454
3. Hong H, Zhang Z, Chung TC, Lee RW (2007) Synthesis of new 1-decene-based LLDPE resins and comparison with the corresponding 1-octene- and 1-hexene-based LLDPE resins. J Polym Sci A 45:639–649
4. van Grieken R, Carrero A, Suarez I, Paredes B (2007) Effect of 1-hexene comonomer on polyethylene particle growth and kinetic profiles. Macromol Symp 259:243–252
5. Kaminsky W, Piel C, Scharlach K (2005) Polymerization of ethene and longer chained olefins by metallocene catalysis. Macromol Symp 226:25–34
6. Sinn HW, Kaminsky W, Vollmer HJ, Woldt R (1983) Preparing ethylene polymers using Ziegler catalyst comprising cyclodienyl compound of zirconium. US Patent 4404344
7. Kaminsky W, Hahnsen H, Kulper K., Woldt R (1985) Process for the preparation of polyolefins. US Patent 4542199
8. Ribeiro MR, Deffieux A, Portela MF (1997) Supported metallocene complexes for ethylene and propylene polymerizations: preparation and activity. Ind Eng Chem Res 36:1224–1237
9. Chien JCW (1999) Supported metallocene polymerization catalysis. Top Catal 7:23–36

10. Kristen MO (1999) Supported metallocene catalysts with MAO and boron activators. Top Catal 7:89–95
11. Hlatky GG (2000) Heterogeneous single-site catalysts for olefin polymerization. Chem Rev 100:1347–1376
12. Jongsomjit B, Kaewkrajang P, Shiono T, Praserthdam P (2004) Supporting effects of silica-supported methylaluminoxane (MAO) with zirconocene catalyst on ethylene/1-olefin copolymerization behaviors for linear low-density polyethylene (LLDPE) production. Ind Eng Chem Res 43:7959–7963
13. Galland GB, Seferin M, Mauler RS, Santos JHZD (1999) Linear low-density polyethylene synthesis promoted by homogeneous and supported catalysts. Polym Int 48:660–664
14. Awudza JAM, Tait PJT (2008) The "comonomer effect" in ethylene/α-olefin copolymerization using homogeneous and silica-supported Cp_2ZrCl_2/MAO catalyst systems: some insights from the kinetics of polymerization, active center studies, and polymerization temperature. J Polym Sci A 46:267–277
15. Li KT, Kao YT (2006) Nanosized silica-supported metallocene/MAO catalyst for propylene polymerization. J Appl Polym Sci 101:2573–2580
16. Li KT, Dai CL, Kuo CW (2007) Ethylene polymerization over a nano-sized silica supported Cp_2ZrCl_2/MAO catalyst. Catal Commun 8:1209–1213
17. Li KT, Ko FS (2008) Dimethylsilylbis(1-indenyl) zirconium dichloride/methylaluminoxane catalyst supported on nanosized silica for propylene polymerization. J Appl Polym Sci 107:1387–1394
18. Chien JCW, He D (1991) Olefin copolymerization with metallocene catalysts. III. Supported metallocene/methyl aluminoxane catalyst for olefin copolymerization. J Polym Sci A 29:1603–1607
19. Atiqullah M, Hammawa H, Hamid H (1998) Modeling the solubility of ethylene and propylene in a typical polymerization diluent: some selected situations. Eur Polym J 34:1511–1520
20. Fogler HS (2006) Elements of chemical reaction engineering, 4th edn. Prentice Hall, Upper Saddle River, NJ, pp 839
21. Zheng X, Smit M, Chadwick JC, Loos J (2005) Fragmentation behavior of silica-supported metallocene/MAO catalyst in the early stages of olefin polymerization. Macromolecules 38:4673–4678
22. Stehling U, Diehold J, Kirsten R, Roll W, Brintzinger H, Jungling S, Mulhaupt R, Langhauser F (1994) ansa-Zirconocene polymerization catalysts with anelated ring ligands – Effects on catalytic activity and polymer chain length. Organometallics 13:964–970
23. McKenna TF, Soares JB (2001) Single particle modelling for olefin polymerization on supported catalysts: a review and proposals for future developments. Chem Eng Sci 56:3931–3949
24. Boor J (1979) Ziegler–Natta catalysts and polymerizations. Academic Press, New York, pp 564
25. Fink G, Richter WJ (1999) Copolymerization parameters of metallocene-catalyzed copolymerizations. In: Brandrup G, Immergut EH, Grulke EA (eds) Polymer handbook, 4th edn. Wiley, New York, pp II-329
26. Green DW, Maloney JO (1997) Perry's chemical engineers' handbook. McGraw-Hill, NY, pp 2–50